Available online at www.sciencedirect.com
ScienceDirect
Journal of Power Sources 177 (2008) 506–511
JOURNAL OF POWER SOURCES
www.elsevier.com/locate/jpowsour

Short communication

Experimental studies on hydrogen generation by methane autothermal reforming over nickel-based catalyst

H.M. Wang *

School of Automotive Engineering, South China University of Technology, Wu Shan Road, Guangzhou 510640, PR China

Received 22 August 2007; received in revised form 10 October 2007; accepted 23 October 2007
Available online 20 December 2007

Abstract

This paper presents the experimental studies on the hydrogen generation by methane autothermal reforming method. An experimental system was built in-house for this study. The temperature profile along the axis of the reformer was measured and discussed. The peak temperature of the reformer appeared in the part of 1/4 to 2/4 of the reformer length from inlet to outlet. The maximum hydrogen yield, hydrogen mole numbers generated per mole of methane consumed of 2.71, was achieved at molar oxygen-to-carbon ratio of 1.68 and molar steam-to-carbon ratio of 2.5. Under this condition, the energy conversion efficiency of the reforming process reached 81.4% based on the lower heating values.

Keywords: Methane; Autothermal reforming; Hydrogen generation; Reaction temperature

1. Introduction

Hydrogen is increasingly regarded as the sustainable fuel of the future and it can be used in combustion devices or fuel cells without any carbon emissions. Since the past two decades, studies on hydrogen generation from various sources, such as fossil fuels, water, biomass, etc. have been extensively reported. Among these, natural gas may be one of the cheapest options for hydrogen generation in the near future [1]. Fuel reforming techniques, including steam reforming (SRF), partial oxidation (POX), catalytic decomposition (CDC), and autothermal reforming (ATR), are usually used to convert natural gas to hydrogen [2]. ATR combining SRF and POX offers advantages for quick transient response and effective suppression of solid carbon formation in the reforming process. Docter and Lamm [3] compared POX, SRF, and ATR systems using gasoline as the feeding stock, and concluded that ATR is the optimum method on the basis of the thermal efficiency under the thermodynamic constraints. Robbins [4] conducted an experimental investigation on ATR of methane (CH_4) by coupling CH_4 catalytic combustion and CH_4 steam reforming in a co-flow heat exchanger where the surface combustion drives the endothermic steam reforming on opposite sides of separating plates in alternating channel flows. The experiments used a flat-plate reactor with simultaneous H_2 or CH_4 combustion over a γ-Al_2O_3-supported Pd catalyst and CH_4 steam reforming over a γ-Al_2O_3-supported Rh catalyst. The results can provide valuable understanding for developing new volumetrically efficient reactor designs for H_2 production using integral catalytic combustion/steam reforming. Liu and Veser [5] studied the influence of the periodicity of flow-reversal, reactor throughput, and catalyst deactivation during catalytic partial oxidation as well as autothermal reforming of methane over noble metal catalysts in a reverse-flow reactor, and measured in situ temperature profiles along the axis of the reactor. They concluded that the use of regenerative heat-integration through dynamic reactor operation yielded reactor configurations, which were ideally suited in particular for small-scale and decentralized hydrogen production from methane.

Studies showed that the commonly used catalysts for the reformation of light hydrocarbons, mainly methane, were Pd-, Ru-, Ni-, Co-, and Fe-based catalysts [6]. The Pt-catalyst on metallic substrate was used in both SRF and ATR of natural gas to generate hydrogen for small-scale stationary fuel cell systems, and thermodynamic equilibrium were nearly reached in these two cases [7]. A catalyst with nickel-free formulation containing

* Tel.: +86 20 88373756; fax: +86 20 87114147.
E-mail address: hmwang123@sina.com.

0378-7753/$ – see front matter © 2007 Elsevier B.V. All rights reserved.
doi:10.1016/j.jpowsour.2007.10.083

precious metals promoted by metal oxides, provided by Johnson Matthey, was used to reform natural gas by the mixture of engine exhaust gas and air using a mini reactor of 1 in. nominal diameter stainless steel tube loaded with two monolith catalysts of 65 mm long and 75 mm long by 25 mm diameter, and 10–15% of hydrogen in the reformate was obtained [8]. Various nickel catalysts were successfully used on the reformation of the natural gas, light hydrocarbons, and methanol to produce hydrogen-rich gas, and the range of working temperatures of nickel catalysts covered from about 450 to 1000 °C [9–11]. Choudhary et al. [11] conducted the experiment of partial oxidation of methane on NiO–ThO_2 and NiO–UO_2 catalysts at 700 and 800 °C, respectively; and Dicks et al. [12] studied steam reformation of methane at 700–1000 °C.

Two main points were emphasized in this paper. Firstly, the temperature profile along the axis of the reformer was measured and the peak temperature was located, which could provide the valuable information for optimization of the design and operation of the reformer; Secondly, a fully instrumented experimental system of methane autothermal reforming was built in-house to validate the theoretical results.

Autothermal fuel reforming combines partial oxidation (POX) and steam reforming (SRF) to achieve a net balance in overall heat of reaction. In this reforming process, the air–fuel and steam–fuel ratios are two important parameters that determine both the reaction temperature and the composition of the reforming products. In our previous thermodynamic analysis of the hydrogen generation from natural gas autothermal reforming [2,13,14], the relationships between the molar air–fuel ratio (A/F) and molar steam–fuel ratio (S/F) and the mole fractions of H_2, CO, and solid carbon in the reformate were obtained, respectively, and the optimum operating conditions in terms of A/F and S/F, under the constraints of maximization of H_2 production, minimization of CO yield, and free from solid carbon in the reforming process, were determined. In this paper, the molar air to methane ratio was expressed as O/C, the molar oxygen-to-carbon ratio based on atomic moles of O in O_2 of air to atomic moles of C in methane, and the molar steam to methane ratio was expressed as S/C, the molar steam-to-carbon ratio based on atomic moles of C in methane. The optimum operating range of O/C of 1.47 and S/C of 2.5–4.0 obtained from our previous thermodynamic study [13] was used to determine the experimental conditions. The experiments were conducted for three S/Cs of 1.0, 2.5, and 3.0, and the O/C range corresponding to a specific S/C was determined by the catalyst working temperature range. In the experiment, different S/Cs and their corresponding O/Cs were obtained by adjusting the feeding flow rates.

2. Experimental

2.1. Experiment system

An experimental system was built in-house for hydrogen generation by methane autothermal reforming in this study. In the autothermal fuel reforming process, hydrogen-rich gas is produced by the reaction of water, fuel, and air. Hence, the reforming system is divided into three parts according to the feeding lines of water, methane, and air. To measure and control the pressures and flow rates of the reactants, the pressure gauges and Cole-Parmer flow control systems with accuracy of ±2% for liquid and ±1% for gas, are installed in these three feeding lines, respectively. Prior to introducing water into the reactor, it is vaporized by a heater. Air, steam, and methane are well mixed in a mixer, pass through a burner, and then enter the reactor where they react over the catalyst to produce the hydrogen-rich gas. The tubular reactor with catalyst bed of length of 200 mm and inner diameter of 60 mm was used in this experiment. The reaction products passing through a cooler, before being discharged to the environment, are extracted to the mass spectrometer to analyze the gas composition. The temperature profile along the axis of the reformer is mapped by 5K-type thermocouples, which are uniformly located along the axis of the catalyst bed. The five thermocouples are very well bonded to a stainless steel sheath to ensure the measuring accuracy within 5 °C. The basic design of the reformer and the locations of the thermal couples are shown in Fig. 1. The catalyst, provided by Engelhard, containing 11% of nickel presented as nickel oxide on a gamma alumina support, was used in this experiment.

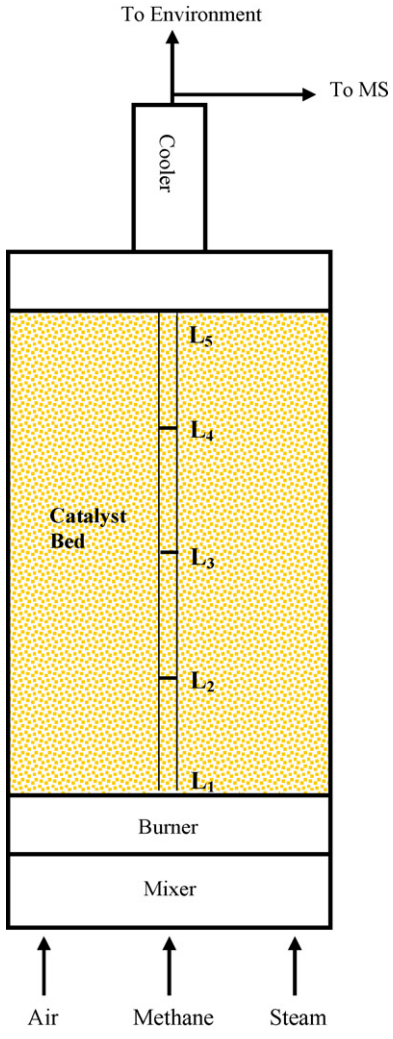

Fig. 1. Basic design of the reformer and temperature measuring points.

2.2. Results and discussion

Autothermal reforming process is composed of exothermic partial oxidation (POX) and endothermic steam reforming (SRF) reactions. The water–gas shift reaction (WGS) also occurs in the process, that is, carbon monoxide reacts with water to form carbon dioxide and hydrogen. The three dominant reactions are:

$$\text{POX}: \ 2CH_4 + (O_2 + 3.76N_2) = 4H_2 + 2CO + 3.76N_2 \quad (1)$$

$$\text{SRF}: \ CH_4 + H_2O = CO + 3H_2 \quad (2)$$

$$\text{WGS}: \ CO + H_2O = CO_2 + H_2 \quad (3)$$

Therefore, the major reforming products from such a general mechanism are H_2, CO, CO_2, non-reacted N_2, H_2O, and CH_4.

The heat balance between exothermic POX and endothermic SRF reactions is achieved for autothermal reforming process. Therefore, the reaction temperature can be controlled by the molar oxygen-to-carbon ratio (O/C) and molar steam-to-carbon ratio (S/C). The increase of O/C leads to the increase of reaction temperature due to the exothermic partial oxidation reaction, and vice versa. For a specific fuel space velocity and S/C, there exists a minimum O/C, below which the reaction temperature will fall abruptly and cause the reformer to go out. It is obvious that the maximum O/C also exists. When O/C is greater than this value, the reaction temperature will rise dramatically and the reformer will run away. During the experiment, the O/C should be controlled between these two values.

2.2.1. Temperature variation along the axis of reformer

Autothermal reforming process consists of three dominant reactions mentioned above, and the total energy balance can be met by matching molar oxygen-to-carbon ratio (O/C) and molar steam-to-carbon ratio (S/C). However, the temperature from inlet to outlet of the reformer is difficult to keep uniform in the experiment, because exothermic partial oxidation reaction is more active than endothermic steam reforming reaction; that is, these two reactions do not occur simultaneously. Therefore, the reaction temperature is usually variable along the reformer. In autothermal reforming process, the peak temperature of the reformer is a very important parameter and should be carefully controlled to prevent the catalyst from overheat. Fig. 2 shows the temperatures measured along the axis of the reformer from start-up to going-out under the condition of S/C of 1.0 and the variation of O/C corresponding to the variation of reaction temperatures. The reaction temperatures were measured by 5 thermocouples, which were uniformly located along the axis of the reformer from the inlet to the outlet (marked by points L_1–L_5, which corresponded to the temperatures referred as T_1–T_5). The O/C of 4.2 was used for methane ignition. The temperatures rose abruptly after ignition at such a high O/C. When T_3 (temperature in point L_3) reached 600 °C, the steam was added into the reactor and at the same time the O/C was adjusted to 1.47, and then followed by 1.26, 1.68, and 0.84. Such a variation of O/Cs could make the reaction temperatures to decrease and increase, and finally caused the reaction to go out. In the ignition stage, there was no reaction in the catalyst bed because all the methane had been burnt out before entering the catalyst bed. The catalyst bed was then heated up by the combustion product. Thus, the temperatures decreased from inlet to outlet of the reformer during this warming up period. When steam was added and O/C was reduced to 1.47, the temperatures decreased. When the catalyst had achieved light off and after the reaction temperature had become stable, the gas temperatures increased from points L_1 to L_2 decreased from L_3 to L_5 and had a little variation between L_2 and L_3. Because at the inlet of the reformer, the concentration of the oxygen was higher and the oxygen was more active than steam, the partial oxidation reaction was dominant from points L_1 to L_2. The whole reaction showed exothermic and hence the temperatures increased in this part. From points L_2 to L_3, the partial oxidation reaction rate decreased due to a decreased concentration of oxygen, but with the increase of temperature, the steam reforming reaction rate increased. The whole reaction achieved the heat balance. That is, the heat released from exothermic reaction was almost equal to the heat absorbed from the endothermic reaction. Therefore, the temperatures exhibited small variation between L_2 and L_3. After point L_3, the exothermic reaction became very weak due to a very small concentration of oxygen. The endothermic reaction became dominant. The whole reaction showed endothermic and hence the temperatures decreased from L_3 to L_5. It can be concluded that in the autothermal reformer, the partial oxidation reaction dominantly occurred in the inlet part of the reformer, the endothermic steam reforming reaction became dominant in the outlet part, and between these two parts, the whole reaction achieved thermo-neutral. Therefore, the peak temperature of the reformer was located between L_2 and L_3 in this autothermal reforming process.

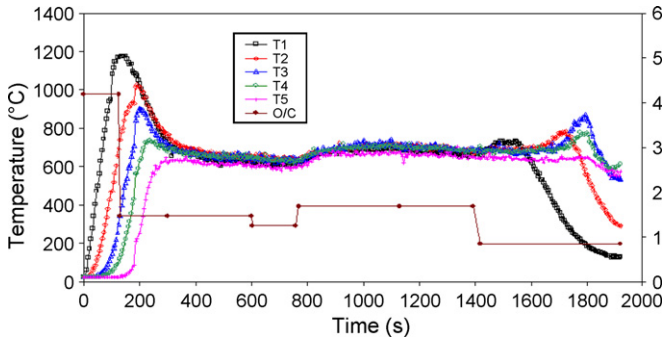

Fig. 2. Temperature profiles along the axis of the reformer from start-up to going-out with a S/C ratio of 1.0 and variable O/C ratios.

Fig. 2 also shows the process of the reformer going out. It can be clearly seen that when the reformer went out, the temperature in L_1 decreased first, and then temperatures in L_2, L_3, L_4, and L_5 decreased in sequence. During the process of the reformer going out, all the temperatures in the reformer showed a small increase before they decreased, because after the upstream of the reformer went out, the oxygen concentration in the downstream would increase, which resulted in a rise of the temperature. However, the temperatures of reactants flowing downstream also sharply decreased, which cooled the catalyst bed. Therefore, the temperatures finally decreased after a small increase, and the reformer went out.

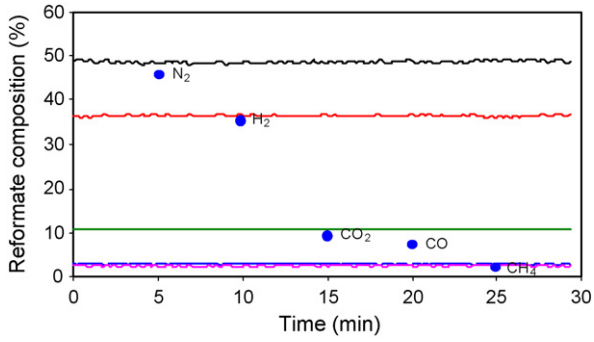

Fig. 3. Composition of the reformate at steady-state operating conditions with O/C of 1.26 and S/C of 1.0.

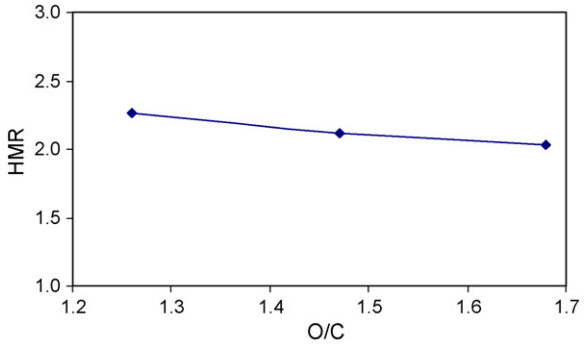

Fig. 5. The relationship between molar hydrogen to methane ratio (HMR) and O/C at S/C of 1.0.

2.2.2. *Molar steam-to-carbon ratio of 1.0*

Methane space velocity was kept to 6740 l/h for the experiments of S/C of 1.0 and corresponding O/Cs, and the values of S/C and O/C were obtained by adjusting flow rates of water and air, respectively. The methane space velocity was defined as

$$S_{\mathrm{M}} = \frac{22.4n}{V_{\mathrm{c}}}$$

where n denoted the molar flow rate of methane in mol/h; V_{c} denoted the catalyst volume in the reformer in L.

During the experiment, it was found that at molar steam-to-carbon ratio (S/C) of 1.0, the reformer could operate at the range of molar oxygen to carbon ratio (O/C) from 1.26 to 1.68 on the condition that the reformer did not go out or run away. Fig. 3 shows the composition of the reformate at the exit of the reformer under steady-state operating conditions for O/C of 1.26 and S/C of 1.0 where the dots represent the reformate composition calculated based on the chemical equilibrium under the same conditions [2,13]. It can be seen that the experimental results fit the theoretical results quite well.

Fig. 4 shows the reaction temperature profiles along the axis of the reformer for O/C of 1.26 and S/C of 1.0. It indicates that the reformer operates very stably under this condition. The average reaction temperature varies from 650 to 690 °C from inlet to outlet of the reformer.

The experiments under O/C of 1.47 and 1.68 were also conducted for S/C of 1.0. Because hydrogen is considered as the only desirable product in the reformate in this study, the hydrogen mole numbers generated per mole of methane consumed, that is, molar hydrogen to methane ratio (HMR), can reflect the energy conversion efficiency of the reforming process. HMR could be obtained by mass balance based on measured feeding flow rates and reformate composition. The bigger the HMR, the higher the energy conversion efficiency will be, and vice versa. Fig. 5 shows the relationship between HMR and O/C for the S/C of 1.0. The HMR decreased with the increase of O/C. The HMR achieved the maximum value of 2.26 ± 0.05 at O/C of 1.26. In this case, the energy conversion efficiency reached $68.1 \pm 1.5\%$.

Fig. 6 shows the variation of average reaction temperatures for S/C of 1.0 and O/C of 1.26, 1.47, and 1.68, respectively. It can be seen that for all O/Cs, the temperatures were increased from points L_1 to L_2 (T_2 is greater than T_1), were decreased from points L_3 to L_5, and show little variation from L_2 to L_3. Such temperature variations suggest that the exothermic and endothermic reactions were dominant at the inlet and outlet of the reformer, respectively, and the whole reaction showed thermo-neutral somewhere between L_2 and L_3.

2.2.3. *Molar steam-to-carbon ratio of 2.5*

Methane space velocity was kept to 2700 L/h for the experiments of S/C of 2.5. When S/C was set to 2.5, the variation range of O/C was from 1.47 to 2.1 on the condition that the reformer could operate stably. Fig. 7 shows the reformate composition for O/C of 1.47 and S/C of 2.5, where the dots represent the

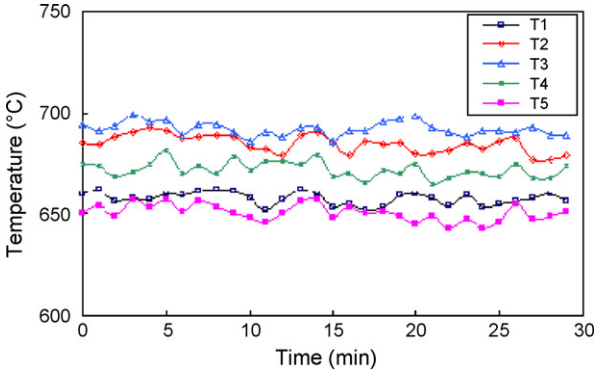

Fig. 4. Reaction temperature profiles along the axis of the reformer at steady-state with an O/C of 1.26 and S/C of 1.0.

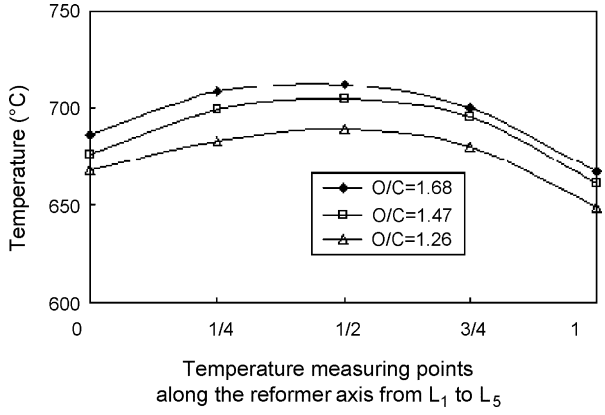

Fig. 6. The average reaction temperature profiles along axis of the reformer (from inlet to outlet) for a S/C of 1.0 and variable O/C ratios.

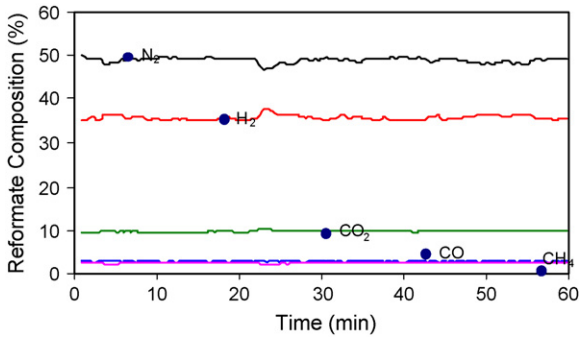

Fig. 7. Reformate composition at S/C of 2.5 and O/C of 1.47.

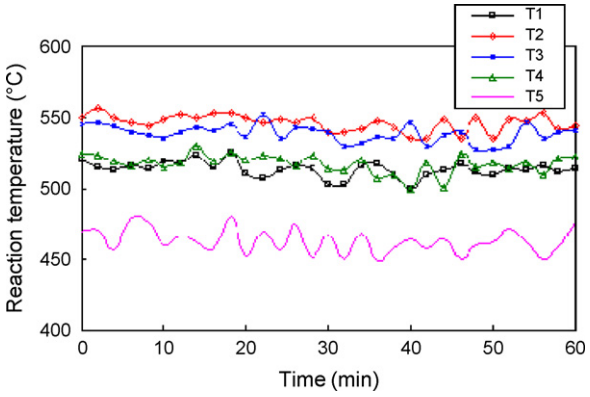

Fig. 8. Reaction temperature profiles along axis of the reformer at S/C of 2.5 and O/C of 1.47.

calculated chemical equilibrium data under the same condition [2,13]. It can be noted that the experimental data and the equilibrium calculation results are in good agreement. The reaction temperature profiles along the axis of the reformer under S/C of 2.5 and O/C of 1.47 are shown in Fig. 8. The reaction temperature varied in the range of 460–550 °C from inlet to outlet of the reformer.

Fig. 9 shows the variation of hydrogen mole numbers generated per mole of fuel consumed, molar hydrogen to methane ratio (HMR), with O/C at S/C of 2.5. The maximum HMR of 2.71 ± 0.08 is achieved at O/C of 1.68. When O/C was smaller than 1.68, more residual methane was found in the reforming product, which resulted in a less hydrogen production. However,

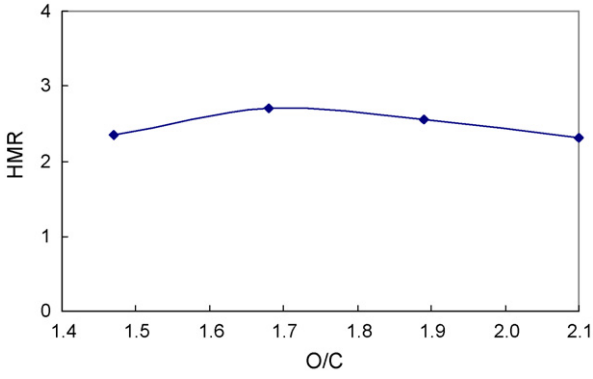

Fig. 9. The relationship between molar hydrogen to methane ratio (HMR) and O/C at S/C of 2.5.

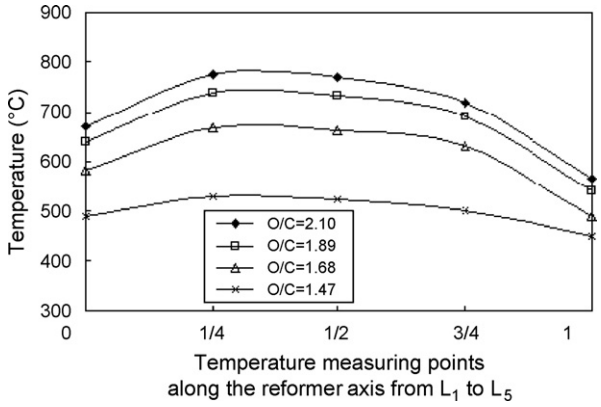

Fig. 10. Average temperature profiles along the axis of the reformer (from inlet to outlet) for S/C of 2.5 and variable O/C ratios.

when O/C was greater than 1.68, the reaction between oxygen and hydrogen might occur, which decreased the final hydrogen production. At O/C of 1.68 and S/C of 2.5, the energy conversion efficiency reached $81.4 \pm 2.4\%$.

Fig. 10 illustrates the average temperature profiles along the reformer under S/C of 2.5 and O/C of 1.47, 1.68, 1.89, and 2.1, respectively. The temperatures were increased from L_1 to L_2 and decreased from L_2 to L_5. The highest reaction temperature (peak temperature) appeared around L_2. With the increase of O/C, the temperature differences between L_2 and other locations of the reformer increased. The reason might be that higher O/C could result in higher peak temperature (appearing at L_2), which increased the endothermic steam reforming reaction rate at the downstream of the reformer.

2.2.4. Discussion

Hydrogen generation by methane autothermal reforming can be used to feed PEM fuel cell, which could be applied in the small-scale stationary power plant. Therefore, H_2 is the most desirable product in the reformate and should be maximized. Solid carbon, on the other hand, is the most undesirable product in the reforming process and once produced, it will deposit on the catalyst surface of the reformer and make the catalyst deactivate. PEM fuel cell usually uses platinum as catalyst. If CO exists in the reformed gas and enters the PEM fuel cell, it will be adsorbed at the platinum catalyst layer of the fuel cell and poison the catalyst. Hence, the reformate needs to be further processed to reduce CO concentration to be less than 10 ppm by a water–gas-shift and preferential oxidation reaction before feeding the PEM fuel cell. Therefore, the focus of the fuel reforming should be placed on maximization of the H_2 yield, minimization of the CO production, and avoiding the formation of solid carbon. Under these constraints, the optimum operating range of O/C of 1.47 and S/C of 2.5–4.0 was obtained from a thermodynamic study [2,13]. However, for an experimental system with specific catalyst, whether a fixed set of O/C and S/C can be achieved depends on if it can make the reaction operate stable and the reaction temperature, especially, the peak temperature of the reformer fall within the range of catalyst working temperature in order to prevent the catalyst from destroy. In this experiment, S/Cs from 1.0 to 4.0 were tested, which covered the

optimum operating range obtained from thermodynamic study. It was found when S/C was set to 3.0, the minimum O/C should be 2.1. In this case, the hydrogen composition in the reformate was about 30%, which was much lower than that for S/C of 1.0 and 2.5. Moreover, too much water was found in the reformate. In practice, the condition of S/C more than 3.0 is not economical for the reformer operation. It is obvious that the maximum hydrogen yield based on hydrogen mole numbers generated per mole of methane consumed was achieved at molar oxygen-to-carbon ratio of 1.68 and molar steam-to-carbon ratio of 2.5 in this experiment, which was approximate to the optimum operating range from theoretical analysis but not completely fall within this range. The reason may be that the reaction temperature was assumed to be uniform in the reactor during calculation, which is different from the experiment condition; that is, the reaction temperature is variable along the reformer. However, the compositions of reforming products for all the sets of O/C and S/C tested in this experiment were in good agreement with those obtained from theoretical analysis. It reveals that chemical equilibrium have been achieved in the experiment.

3. Conclusions

In this study, an in-house experimental system was fabricated for autothermal methane reforming to produce hydrogen-rich gas, and the theoretical results were successfully validated. The chemical equilibrium was nearly reached in all the tested conditions. The maximum hydrogen yield, hydrogen mole numbers generated per mole of methane consumed of 2.71 ± 0.08, was achieved at molar oxygen-to-carbon ratio of 1.68 and molar steam-to-carbon ratio of 2.5. Under this condition, the energy conversion efficiency reached $81.4 \pm 2.4\%$ on a lower heating value basis.

The temperature profile along the axis of the reformer was measured, and the peak temperature of the methane autothermal reforming process appeared around the location of 1/4–2/4 of the reformer length from the inlet of the reformer. These results are important for optimization of the design and operation of the autothermal reformer.

Acknowledgement

Financial assistance obtained from the national natural science foundation of China, numbered as 50776036, is gratefully acknowledged.

References

[1] C.-J. Winter, Int. J. Hydrogen Energy 29 (11) (2004) 1095–1097.
[2] W. Hongmin, Theoretical and experimental investigations of fuel reforming for fuel cell applications, Ph.D. thesis, 2002, Nanyang Technological University.
[3] A. Docter, A. Lamm, J. Power Sources 84 (2) (1999) 194–200.
[4] A. Robbins Fletcher, H. Zhu, S. Jackson Gregory, Catal. Today 83 (2003) 141–156.
[5] T. Liu, G. Veser, AIChE Annual Meeting, Conference Proceedings, 05AIChE, AIChE Annual Meeting and Fall Showcase, Conference Proceedings, 2005, p. 10006.
[6] K. Ledjeff-Hey, V. Formanski, T. Kalk, J. Roes, J. Power Sources 71 (1/2) (1998) 199–207.
[7] A. Heinzel, B. Vogel, P. Hubner, J. Power Sources 105 (2002) 202–207.
[8] D. Yap, S.M. Peucheret, A. Megaritis, M.L. Wyszynski, H. Xu, Int. J. Hydrogen Energy 31 (2006) 587–595.
[9] M.G. Gonzalez, N.N. Nichio, B. Moraweck, G. Martin, Mater. Lett. 45 (12000) (2000) 15–18.
[10] M.L. Praharso, D.L. Trimm, Mater. Sci. Forum 315 (1999) 187–193.
[11] V.R. Choudhary, A.M. Rajput, B. Prabhakar, A.S. Mamman, Fuel 77 (15) (1998) 1803–1807.
[12] A.L. Dicks, K.D. Pointon, A. Siddle, J. Power Sources 86 (1) (2000) 523–530.
[13] S.H. Chan, H.M. Wang, Int. J. Hydrogen Energy 25 (2000) 441–449.
[14] S.H. Chan, H.M. Wang, Fuel Process. Technol. 64 (2000) 221–239.